JOURNAL OF CATALYSIS 145, 377–383 (1994)

Chemical Vapor Deposition of Platinum Hexafluoroacetylacetonate inside KL Zeolite: A New Route to Nonacidic Platinum-in-Zeolite Catalysts

Carlo Dossi,* Rinaldo Psaro,*,[1] Andrea Bartsch,* Achille Fusi,* Laura Sordelli,* Renato Ugo,* Maurizio Bellatreccia,† Roberto Zanoni,† and Gilberto Vlaic‡

*Dipartimento di Chimica Inorganica, Metallorganica e Analitica and Centro CNR, Università di Milano, Milan, Italy; †Dipartimento di Chimica, Università "La Sapienza," Rome Italy; and ‡Dipartimento di Scienze Chimiche, Università di Trieste, e Sincrotrone Trieste ScpA, Trieste, Italy

Received March 8, 1993; revised June 24, 1993

Platinum hexafluoroacetylacetonate can be selectivity introduced inside KL zeolite channels via CVD in a flow of Ar at 70°C. Metal particles are then formed via thermal removal of the volatile organic ligands under H_2 at 350°C. *In situ* DRIFTS and EXAFS measurements suggest the formation of very small Pt clusters with a nucleophilic character. These nonacidic Pt/KL catalysts show remarkably high activity and selectivity in the conversion of methylcyclopentane to benzene at 500°C. A long catalyst life is achieved due to reduced coke formation and a very slow sintering rate. © 1994 Academic Press, Inc.

INTRODUCTION

The remarkable activity and stability of Pt/KL catalysts for the selective aromatization of linear hydrocarbons to aromatics have attracted considerable interest in recent years (1, 2). Their unique catalytic behvior is thought to be directly related to the geometric and electronic properties of small Pt particles located inside the linear channels of L zeolite (2–4). Moreover, any acidity introduced during the preparation and/or activation steps is greatly detrimental to the selectivity and stability of the catalyst (5).

In principle, the conventional ion-exchange technique is to be avoided in the preparation of zeolite-entrapped Pt particles, since acidity is inherently generated upon hydrogen reduction (6). Consequently, several other methodologies have been used, involving incipient wetness impregnation, as well as neutralization of acid sites following ion exchange, and the use of modifiers, such as KCl, as acidity scavengers (7).

The problem of obtaining nonacidic metal-in-zeolite catalysts has recently been approached in a completely different way, using neutral organometallic complexes as metal precursors. The organometallic molecule can be selectively introduced into zeolite cages via chemical vapor deposition (CVD), without altering the distribution of intrazeolitic cations. Metal particles are then simply formed via thermal removal of the volatile ligands under reducing conditions (8, 9).

Pt/K–LTL zeolite catalysts have been the object of a series of detailed X-ray absorption spectroscopy studies performed by different authors (10–12). These studies have given a great deal of information about dimensions, morphology, and metal–support interaction of the particles (13–15).

In this paper, we describe the preparation, characterization, and EXAFS investigation of nonacidic Pt/KL catalysts obtained via CVD of platinum hexafluoroacetylacetonate. Methylcyclopentane conversion is chosen as a model reaction with which to investigate the nature of the active sites of small Pt clusters inside the zeolite channels.

EXPERIMENTAL

Catalyst Preparation

Platinum hexafluoroacetylacetonate [$Pt(hfa)_2$] (Strem Chemicals, Inc.) was purified twice by sublimation in inert atmosphere. KL zeolite (Linde Type L, batch no. 961687040007) was purchased from UOP, Linde Division. It is characterized by a unidimensional network of parallel channels with a diameter of 7.1 Å.

The deposition of the organometallic precursor was carried out in a glass "U" tube, fitted with a quartz frit and greaseless stopcocks. The zeolite was placed on the frit and heated in an argon flow (ca. 10 ml/min) from 25 to 400°C over 2 h in order to remove physisorbed water. After cooling to room temperature, the organometallic precursor was introduced into the flow of argon (2 ml/min) at the bottom of the "U" tube. The reactor was

[1] To whom correspondence should be addressed.

0021-9517/94 $6.00

heated to the sublimation temperature (70°C) in the flow of argon for the time required to effect complete deposition of the organometallic complex [Pt(hfa)$_2$] (9). The subsequent decomposition to metal was performed in hydrogen atmosphere at 350°C for 1 h.

In all samples, the metal loading was about 1 wt%, as measured by atomic absorption spectroscopy.

Temperature-Programmed Studies

The kinetics of thermal decomposition to metal of [Pt(hfa)$_2$]/KL was studied by temperature-programmed reductive decomposition (TPRD). The supported material was heated in H$_2$(5%)/He flow from ambient temperature to 500°C with a heating rate of 3°C/min. The volatile decomposition products were then detected downstream in the carrier gas as a function of increasing temperature by an on-line quadrupole mass spectrometer (VG Masstorr, 1–100 amu).

Temperature-programmed oxidation (TPO) of coke residues after the catalytic run has been performed under similar conditions. An O$_2$(2%)/He mixture was flowed over the catalyst and the evolved CO$_2$ was detected via an on-line gas chromatograph (Intersmat IGC 12) equipped with a FID and a methanation converter (16).

Catalytic Studies

Methylcyclopentane (MCP) conversion was performed between 350 and 500°C on a continuous-flow, fixed-bed microreactor, working at atmospheric pressure, with an H$_2$/MCP ratio of about 20. Product analysis was carried out by an on-line gas chromatograph (Carlo-Erba Instruments HRGC 5160) using a 50-m, 0.2-mm cross-linked methylsilicone (Hewlett–Packard PONA) capillary column.

Diffuse Reflectance Infrared Spectroscopy

Metal aggregates inside the zeolite cages were investigated by *in situ* diffuse reflectance infrared Fourier transform spectroscopy (DRIFTS) on a FTS-40 Digilab spectrophotometer fitted with a Harrick DRA-2CI diffuse reflectance attachment and a Harrick HVC cell, which allows one to record the spectra of the sample in granular form under controlled temperature and pressure conditions.

DRIFTS measurements of CO adsorbed on Pt particles were carried out at atmospheric pressure in CO flow at room temperature immediately after the reduction in H$_2$ flow at 450°C.

All spectra were recorded at 4 cm^{-1} resolution with the coaddition of 100 scans per spectrum and were converted into the Kubelka–Munk reflectance form using the KBr spectrum as a reference.

EXAFS Measurements

EXAFS measurements were carried out at the DCI storage ring at LURE (Orsay, France). Measurements were taken in transmission mode, with an Si(111) channel-cut monochromator and two ion chambers filled with air. Spectra were recorded at the Pt L_{III} edge (11,564 eV) over a range of 700 eV, with an experimental resolution of 2 eV, and counting time of 1.5 s.

All *ex situ* mounted samples were prepared immediately before the measurements, transferred in air-tight containers filled with Ar, handled in a glove-box under flowing argon, and mounted in the holder of an *in situ* cell, which allows heating from room temperature to 600°C under controlled atmosphere.

EXAFS measurements were performed on the following samples:

(i) after sublimation of [Pt(hfa)$_2$] inside KL zeolite.

(ii) after reduction of [Pt(hfa)$_2$]/KL in the EXAFS cell, performed by heating under H$_2$ from 25 to 350°C, at a heating rate of 3°C/min, and then left at 350°C for 1 h.

(iii) after *ex situ* H$_2$ reduction, with the procedure outlined in (ii), followed by a catalytic test of MCP conversion at 500°C and 1 atm for 2 h.

EXAFS Data Analysis

Due to the low Pt loading (1%), all EXAFS spectra were successively acquired at least three times under the same experimental conditions and averaged before data analysis.

The EXAFS $\chi(k)$ signal was extracted from absorption data by a conventional procedure outlined below. A linear background was fitted in the pre-edge region and extrapolated to higher energies. The atomic-like absorption contribution, estimated by a polynomial fit, was subtracted from the experimental data and the result was normalized to edge height, to give the experimental $\chi(k)$. The k^3-weighted $\chi(k)$'s were Fourier-transformed over a Kaiser window of 30–650 eV. A Fourier filtering was then applied in order to extract Pt nearest neighbor shells. These shells were modeled by a nonlinear least-squares routine, which computes coordination numbers (N), bond lengths (R), and Debye–Waller-like factors ($\Delta\sigma^2$) (17). In this process we made use of the theoretical backscattering amplitudes and phase shifts calculated by McKale *et al.* (18).

RESULTS AND DISCUSSION

Deposition of [Pt(hfa)$_2$] inside KL Zeolite

The preparation of heterogeneous metal catalysts via CVD (9) requires the utilization of thermally stable and volatile organometallic complexes with proper dimensions to fit into the pores of the zeolite structure. These

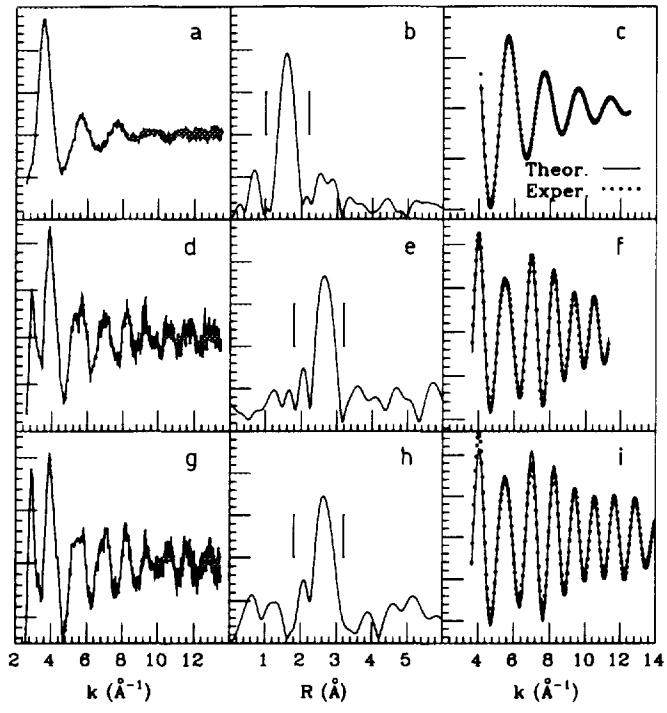

FIG. 1. Experimental $\chi(k)$'s, k^3-weighted Fourier transforms, and corresponding filtered first shell contribution of $[Pt(hfa)_2]/KL$ inside zeolite channels (a–c), after H_2 reduction (e, f), and after catalytic test at 500°C (g, i). Vertical bars indicate filtered range.

conditions severely limit the choice of suitable platinum organometallic compounds. The square-planar hexafluoroacetylacetonate complex, $[Pt(hfa)_2]$, was found to fulfill the above requirements.

A proper choice of the CVD conditions, in particular the sublimation rate, is of primary importance for maximizing the deposition yield (9). The rate of diffusion of the organometallic precursor inside zeolite channels is necessarily slow, because of the geometrically constrained environment of the zeolite structure. Moreover, the precursor molecule is entrapped within the channels of the support via nonbonding interactions with the oxygen ions and/or the zeolite cations. In fact, no zeolitic protons and/or reactive –OH groups are left inside channels of KL zeolites.

An EXAFS investigation was carried out on a freshly sublimed sample of $[Pt(hfa)_2]$ on KL zeolite, in order to verify the selective deposition of the precursor inside the cages and to provide evidence for the stability of the organoplatinum molecule inside the zeolite. Experimental $\chi(k)$'s, the Fourier transform, and the first shell filtered contribution are shown in Figs. 1a–1c.

The modulus of the Fourier transform of the k^3-weighted EXAFS experimental data obtained from the Pt L_{III} edge absorption spectrum of the above sample shows one prominent feature at ~1.5 Å (without correction for the phase shift) (Fig. 1b).

The amplitude of the remaining features is comparable with the noise level, possibly because the experimental signal from outer shells derives from light elements such as carbon and fluorine, which have limited scattering power.

The results of the analysis performed on the Fourier-filtered first shell (Fig. 1c) give four oxygen atoms at a mean distance of 1.98 Å. These values closely agree with X-ray diffraction data for the analogous $[Pt(acac)_2]$ [acac = acetylacetonate] complex ($N = 4$, $R = 1.99$ Å) (19). The retention of the original structure of the precursor upon deposition inside the zeolite cages is thus confirmed. The absence of Pt–Pt coordination shells suggests that no metal aggregation is present at this preparation stage.

The microporous network of L-type zeolite appears to be a basic requirement for allowing the preferential entrapping of $[Pt(hfa)_2]$ without modifications of the original molecular structure.

Thermal Decomposition to Entrapped Metal Particles

The kinetics of the thermal decomposition of the organometallic precursor to metal have been investigated by temperature-programmed reductive decomposition (TPRD). The TPRD profile of $[Pt(hfa)_2]/KL$ in $H_2(5\%)$/He is shown in Fig. 2. The evolution of hexafluoroacetylacetone (Hhfa) takes place in a main peak at 265°C, according to a one-step mechanism of reductive elimination of ligands,

$$[Pt(hfa)_2]/KL \xrightarrow{H_2} 1/x\ Pt_x/KL + 2\ Hhfa,$$

which leads to metallic platinum. The presence of the small shoulder at 190°C can be interpreted as the presence

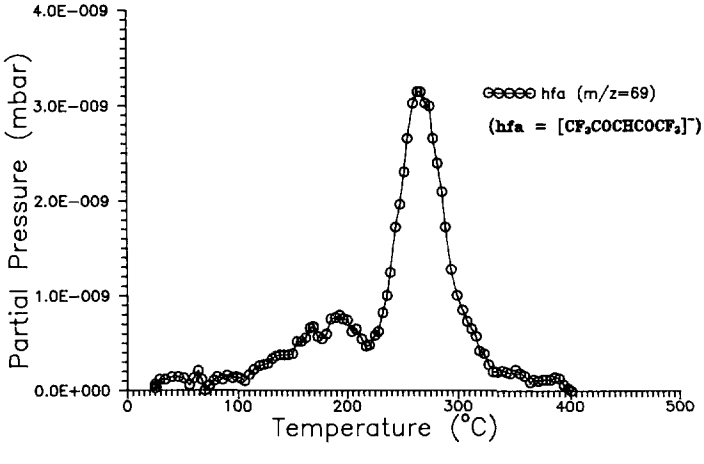

FIG. 2. TPRD profile in flow of H_2/He mixture of $[Pt(hfa)_2]/KL$.

TABLE 1

Structural Parameters Obtained by a Nonlinear Fit Procedure Performed on Experimental EXAFS First Shell Filtered Data of Pt/KL Catalyst

	Shell	N	R (Å)	σ^2(× 10^{-2} Å^2)
After sublimation in zeolite KL	Pt–O	4 ± 1	1.98 ± 0.02	5.8 ± 0.5
After H_2 reduction at 350°C	Pt–Pt	5 ± 1	2.76 ± 0.02	7.1 ± 0.7
After catalytic test at 500°C	Pt–Pt	6 ± 1	2.76 ± 0.02	8.6 ± 1.0
$N(13)_{cuboct}$[a]		5.56		
$N(13)_{icos}$[a]		6.46		

[a] $N(13)_{cuboct}$ and $N(13)_{icos}$ indicate calculated mean coordination numbers for 13-atom cuboctahedral and icosahedral structures, respectively (21).

of the [Pt(hfa)$_2$] precursor in a different location of the zeolite channels. No deposition of the precursor is observed on the external surface, since the decomposition temperature is about 130–200°C higher than that required for vapor deposition. No metal leaching was observed during the reduction process, as confirmed by AAS measurements.

The formation of zeolite-entrapped small metallic particles upon thermal removal of Hhfa ligands has been confirmed by *in situ* EXAFS experiments. The full $\chi(k)$ signal extracted from the Pt/KL sample obtained by *in situ* thermal decomposition in H_2 of [Pt(hfa)$_2$] is shown in Fig. 1d, together with its Fourier transform (e) and first shell filtered contribution (f).

The Fourier transform shows a relevant contribution located close to the distance expected for the first coordination shell of Pt foil. Evidence for nonnearest neighbor shells cannot be confidently claimed. The first shell filtered contribution of the reduced sample is similar to the corresponding contribution from Pt foil, with reduced amplitude. On the same shell a fit was performed, resulting in a coordination distance (Table 1) which reproduces, within experimental error, the Pt–Pt bulk value (R = 2.77 Å). The corresponding Pt–Pt coordination number is, however, much smaller than that for bulk Pt (N = 12), whereas the Debye–Waller factor compares with that of bulk Pt. The picture emerging from the above results is again in favor of the metal content of the sample being constituted by small Pt particles. In the range of distances in which typical metal–oxygen bond lengths for supported samples are found (11), no Pt–O coordination shell was observed in our sample. A similar situation was observed by McHugh *et al.* (10) in an EXAFS experiment performed on a Pt–MgKL ion-exchanged sample.

In the absence of accurate information about the nonnearest coordination shell, a discussion of the structure of the particles is impractical. In order to give an estimate of the Pt particle mean diameter and nuclearity, we compare in Table 1 experimental first shell Pt–Pt mean coordination numbers with the corresponding ones for ideal cubo-octahedral and icosahedral structures (20). These two structures have been widely proposed as suitable geometrical models for small metal clusters (21). From a comparison of experimental and calculated mean coordination numbers, an upper limit of 14–15 atoms per particle can be set, corresponding to a maximum particle diameter of 7–8 Å.

The process of reduction to metallic platinum, following the complete removal of the organic ligands, has also been monitored by *in situ* DRIFTS. We have used CO as a probe molecule for studying the state of Pt particles entrapped in zeolite channels. CO was flowed through the DRIFT cell at room temperature. The spectrum, recorded after a 5-min purge in inert atmosphere (Fig. 3), shows peaks in the ν(CO) region at 2042(m), 2004(vs), 1965(s), and 1866(w) cm^{-1}. The fine structure of the spectrum and the location of the carbonyl bands suggest the formation of carbonyl cluster anions similar to those synthesised by Longoni and co-workers (22) in basic solution, of general

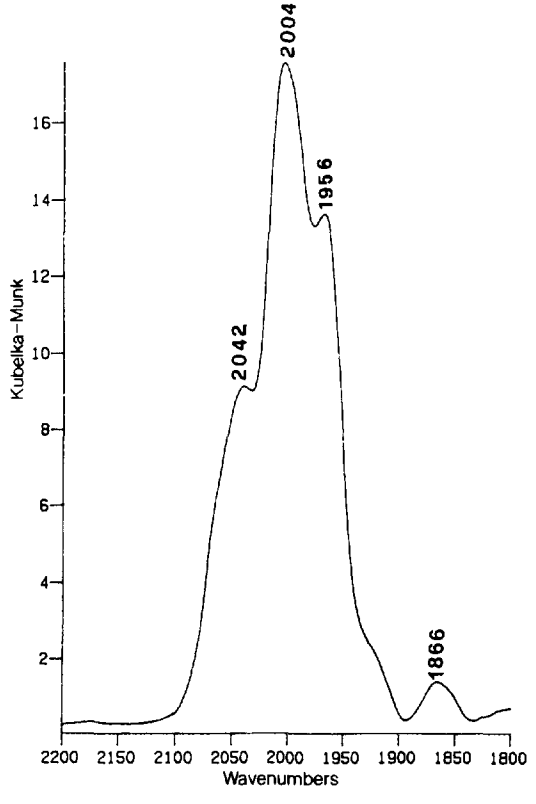

FIG. 3. DRIFT spectrum, in the ν(CO) region, of CO adsorbed on prereduced Pt/KL.

TABLE 2

Total Activity and Product Selectivity in MCP Re-forming at 350°C and 1 atm with Pt/KL Catalysts

Time on stream (min)	Total conversion (mol%)	Selectivity[a] RO	BZ (mol%)	CRACK
5	23	95.5	3.2	1.3
60	29	94.7	3.3	2.0

[a] RO, ring opening; BZ, benzene; CRACK, cracking.

formula $[Pt_3(CO)_6]_n^{2-}$ (n = 1–4). Similar IR spectra attributed to carbonylated Pt clusters in basic zeolites have been observed by different authors (23). Thermochemical and spectroscopic data clearly indicate the formation of very small Pt clusters embedded in the framework with a small number of Pt atoms. Upon adsorption of CO they would give rise to the carbonyl cluster anions. From an electronic point of view, the Pt particles have an excess electron density, which we call electron-rich character. This effect on the Pt state is induced by the basic sites of zeolite KL (e.g., the interaction of some Pt atoms of a particle with the negatively charged framework oxygen atoms) (24).

This evidence discounts any possibility that acidic sites are formed upon reduction of the organometallic complexes introduced via CVD, as observed instead when metal precursor is introduced via ion exchange.

Catalytic Activity

The presence of acidity in the close proximity of metal particles has been demonstrated to play a fundamental role in the catalytic activity and selectivity of zeolite-entrapped metal catalysts for hydrocarbon conversion. Following the work of Bai and Sachtler (25), methylcyclopentane conversion was chosen as a model reaction with which to investigate the nature of the active sites in platinum catalysts obtained by CVD.

TABLE 3

Ring Opening Selectivity in MCP Conversion at 350°C and 1 atm with Pt/KL Catalysts

Product ratio	Selectivity Statistical (mol%)	Observed (mol%)
n-Hexane	40	34
3-Methylpentane	20	27
2-Methylpentane	40	39

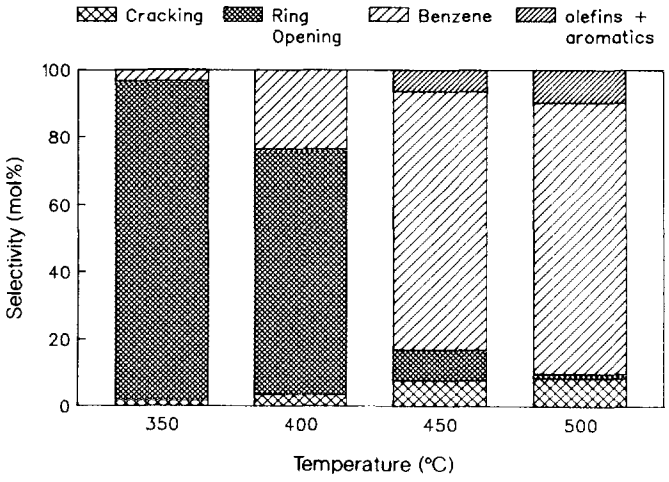

FIG. 4. Product selectivity in MCP conversion as a function of temperature with Pt/KL catalyst.

Total activity data of Pt/KL catalysts in MCP conversion at 350°C and 1 atm are shown in Table 2 as a function of time on stream. In addition, the product selectivity after 30 min on stream indicates that mainly ring opening (RO) products (methyl-2-pentane, methyl-3-pentane, and n-hexane) are formed, together with small amounts of cyclopentane, via demethylation of MCP. The relative ratios of the three RO products (Table 3) deviate significantly from those expected on the basis of a statistical rupture of the MCP molecule, as was observed for small Pt particles deposited on amorphous supports (26).

A geometrical interpretation has been proposed to explain the observed stereoselectivity (27), involving: (i) the preferential orientation of the MCP molecule with its long axis parallel to the channel axis of the pores of L zeolite, where the Pt clusters are located; and (ii) rollover limitations of the adsorbed MCP molecule, thus causing a nonequivalence of the two faces of the molecule.

This explanation, however, is assumed to be valid only in the absence of coke deposits poisoning the metal surface. It is nevertheless true that a monofunctional mechanism does not reasonably offer any easy pathway toward the formation of hard coke (28). Accordingly, no significant CO_2 evolution, particularly above 300°C, is observed in TPO analysis on a used catalyst after 5 h on stream.

The unique properties of Pt/KL catalysts, i.e., activity and selectivity to benzene formation, are exploited at higher temperatures (Fig. 4). On raising the temperature, the selectivity to benzene steadily increases at the expense of ring opening and is by far the preferred reaction at 500°C. According to the widely accepted approach of Tamm *et al.* (1), benzene cannot derive directly from MCP, but must arise instead via dehydro,1-6,-cyclization of n-hexane formed by ring opening of MCP. When the ring opening product distribution is plotted against tem-

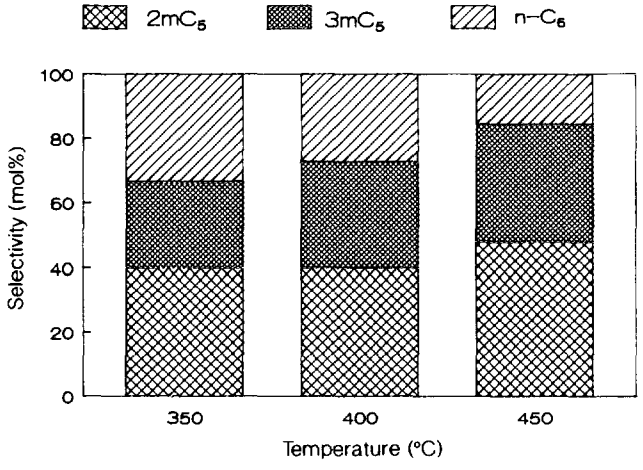

FIG. 5. Ring opening selectivity in MCP conversion as a function of temperature with Pt/KL catalyst.

perature (Fig. 5), it is immediately evident that *n*-hexane is preferentially depleted with respect to the other two isomers, 2- and 3-methylpentane, which cannot give 1–6 cyclization. It should also be noted that, at 500°C, both total activity and benzene selectivity are constant for over 18 h on stream.

This behavior can be related to the results obtained from an EXAFS experiment performed on a Pt/KL sample after catalytic test (see Experimental). Experimental $\chi(k)$'s, the Fourier transforms F(R), and first shell filtered contribution are shown in Figs. 1g–1i.

Pt–Pt coordination number and bond length (Table 1) can be compared with those obtained from the EXAFS analysis performed on Pt/KL sample after H_2 reduction. The experimentally observed equivalence of metal nuclearities and estimated diameters in both cases support the hypothesis of the confinement of metal particles inside KL-zeolite cages. This is in close agreement with molecular graphics simulations, which allow a Pt_{15} particle to ideally fit into an LTL cage (3).

No evidence of Pt–C contribution was experimentally observed, confirming the absence of a significant coke deposition on the metal surface, already suggested by TPO.

In summary, the special catalytic behavior of these organometallic-based Pt/KL catalysts is related to the formation and stabilization of very small Pt_n clusters inside zeolite channels. The cluster–cage interaction seems to provide the Pt clusters with electron-rich character.

This might also explain the particular resistance of these organometallic-based catalysts to sintering and coke deposition. Preliminary investigations indicate that working Pt/KL catalysts can be easily and effectively regenerated under an oxygen atmosphere, with an almost complete restoration of the original catalytic activity and selectivity.

CONCLUSIONS

Chemical vapor deposition of $[Pt(hfa)_2]$ is proposed as an emerging methodology for the preparation of nonacidic Pt/KL catalysts. The organometallic precursor is easily introduced inside the KL zeolite without perturbing the cation distribution throughout the cages, thus preventing the formation of protons upon reduction. Small Pt clusters, with an electron-rich character, are easily formed under reducing conditions.

All the traditional steps in catalyst preparation, viz., drying, calcination, and reduction, which critically affect catalyst performance, can be eliminated. Reduction and activation of the catalyst can be simultaneously carried out in the reactor before the catalytic run. Remarkably high activity and selectivity in MCP conversion to benzene are observed, with a long catalyst life due to reduced coke formation and a very slow sintering rate.

ACKNOWLEDGMENTS

This work has been done under a "Progetto Finalizzato Chimica Fine" of the Italian National Research Council (CNR). Support from NATO (Research Grant 900056) in collaboration with Professor W. M. H. Sachtler (Evanston, IL) and Professor H. Knözinger (Munich, Germany) is gratefully acknowledged. M.B. gratefully acknowledges a fellowship from Enricherche. EXAFS measurements at LURE were financially supported by the EEC through the "Large Installations Plan." We gratefully acknowledge Ms. F. Villain for assistance at LURE.

REFERENCES

1. Tamm, P. W., Mohr, D. H., and Wilson, C. R., *in* "Catalysis 1987" (J. W. Ward, Ed.), p. 335. Elsevier, Amsterdam, 1988.
2. Tauster, S. J., and Steger, J. J., *Mater. Res. Soc. Symp.* **111,** 419 (1988).
3. Derouane, E. G., and Vanderveken, D., *Appl. Catal.* **45,** L15 (1988).
4. Hong, S. B., Mielczarski, E., and Davis, M. E., *J. Catal.* **134,** 349 (1992); Mielczarski, E., Hong, S. B., Davis, R. J., and Davis, M. E., *J. Catal.* **134,** 359 (1992); Mielczarski, E., Hong, S. B., and Davis, M. E., *J. Catal.* **134,** 70 (1992).
5. Alvarez, W. E., and Resasco, D. E., *Catal. Lett.* **8,** 53 (1991).
6. Chow, M., Park, S. H., and Sachtler, W. M. H., *Appl. Catal.* **19,** 349 (1985).
7. Ostgard, D. J., Kustov, L., Poeppelmeier, K. R., and Sachtler, W. M. H., *J. Catal.* **133,** 342 (1992).
8. Dossi, C., Schaefer, J., and Sachtler, W. M. H., *J. Mol. Catal.* **52,** 193 (1989).
9. Dossi, C., Bartsch, A., Galasco, A., Losi, P., and Psaro, R., *Catal. Today* **17,** 527 (1993).
10. McHugh, B. J., Larsen, G., and Haller, G. L., *J. Phys. Chem.* **94,** 8621 (1990).
11. Vaarkamp, M., Grondelle, J. V., Miller, J. T., Sajkowsky, A. J., Modica, F. S., Lane, G. S., Gates, B. C., and Konigsberger, D. C., *Catal. Lett.* **6,** 369 (1990).
12. Larsen, G., and Haller, G. L., *Catal. Today* **15,** 431 (1990).
13. Larsen, G., and Haller, G. L., *Catal. Lett.* **3,** 103 (1989).
14. Li, G.-J., Fujimoto, T., Fukuoka, A., and Ichikawa, M., *Catal. Lett.* **12,** 171 (1992).
15. Koningsberger, D. C., and Gates, B. C., *Catal. Lett.* **14,** 271 (1992).

16. Dossi, C., Fusi, A., *Anal. Chim. Acta* **217,** 197 (1989).
17. Michalowicz, A., *in* "Logiciels pour la Chimie," pp. 102–103. Société Française de Chimie, Paris, 1991.
18. McKale, A. G., Veal, B. W., Paulikas, A. P., Chan, S. K., and Knapp, G. S., *J. Am. Chem. Soc.* **110,** 373 (1988).
19. Katoh, M., Miki, K., Kai, Y., Tanaka, N., and Kasai, N., *Bull. Chem. Soc. Jpn.* **54,** 611 (1981).
20. Fritsche, H. G., and Benfield, R. E., *Z. Phys. D* **26,** 515 (1993).
21. Montano, P. A., Shenoy, G. K., Alp, E. E., Schulze, W., and Urban, J., *Phys. Rev. Lett.* **56,** 2076 (1986).
22. Longoni, G., and Chini, P., *J. Am. Chem. Soc.* **98,** 7225 (1976); Chini, P., Longoni, G., and Albano, V. G., *Adv. Organomet. Chem.* **14,** 285 (1976).
23. Li, G.-J., Fujimoto, T., Fukuoka, A., and Ichikawa, M., *Catal. Lett.* **12,** 171 (1992); Bischoff, H., Jaeger, N. I., Schulz-Ekloff, G., and Kubelkova, L., *J. Mol. Catal.* **80,** 95 (1993); Besoukhanova, C., Guidot, J., Barthomeuf, D., Breysse, M., and Bernard, J. R., *J. Chem. Soc. Faraday Trans. 1* **77,** 1595 (1981); Chang, J.-R., Xu, Z., Purnell, S. K., and Gates, B. C., *J. Mol. Catal.* **80,** 49 (1993); De Mallmann, A., and Barthomeuf, D., *Catal. Lett.* **5,** 293 (1990).
24. De Mallmann, A., and Barthomeuf, D., *in* "Zeolites as Catalysts, Sorbents and Detergent Binders" (H. G. Karge and J. Weitkamp, Eds.). Elsevier, Amsterdam, 1989.
25. Bai, X., and Sachtler, W. M. H., *J. Catal.* **129,** 121 (1991).
26. Gault, F. G., *Adv. Catal.* **30,** 1 (1981).
27. Moretti, G., and Sachtler, W. M. H., *J. Catal.* **116,** 350 (1989).
28. Augustine, S. M., Alameddin, G. N., and Sachtler, W. M. H., *J. Catal.* **115,** 217 (1989).